Gene therapy targeting the inner retina rescues the retinal phenotype in a mouse model of CLN3 Batten disease

Short title (50 characters): Gene therapy targeting the inner retina in CLN3 disease

Sophia-Martha kleine Holthaus[1], Mikel Aristorena[1], Ryea Maswood[1], Olha Semenyuk[1], Justin Hoke[1], Aura Hare[1], Alexander J. Smith[1], Sara E. Mole[2,3,4], and Robin R. Ali[1,5]

[1]Department of Genetics, UCL Institute of Ophthalmology, 11-43 Bath Street, London EC1V 9EL, UK

[2]MRC Laboratory for Molecular Cell Biology, University College London, Gower Street, London WC1E 6BT, UK

[3]UCL Institute of Child Health, 30 Guildford Street, London WC1N 1EH, UK

[4]UCL Department of Genetics, Evolution and Environment, University College London, Gower Street, London WC1E 6BT

[5]NIHR Biomedical Research Centre at Moorfields Eye Hospital NHS Foundation Trust

Corresponding author:

Robin Ali, UCL Institute of Ophthalmology, 11-43 Bath Street, London EC1V 9EL, UK, email: r.ali@ucl.ac.uk, phone: +44-207-608-6817

Abstract (300 words)

The neuronal ceroid lipofuscinoses (NCLs), often referred to as Batten disease, are inherited lysosomal storage disorders that represent the most common neurodegeneration during childhood. Symptoms include seizures, vision loss, motor and cognitive decline and premature death. The development of brain-directed treatments for NCLs has made noteworthy progress in recent years. Clinical trials are currently ongoing or planned for different forms of the disease. Despite these promising advances, it is unlikely that therapeutic interventions targeting the brain will prevent loss of vision in patients as retinal cells remain untreated and will continue to degenerate. Here, we demonstrate that *Cln3*$^{\Delta ex7/8}$ mice, a mouse model of CLN3 Batten disease with juvenile onset, suffer from a decline in inner retinal function resulting from the death of rod bipolar cells, interneurons vital for signal transmission from photoreceptors to ganglion cells in the retina. We also show that this ocular phenotype can be treated by adeno-associated virus (AAV)-mediated expression of *CLN3* in cells of the inner retina, leading to significant survival of bipolar cells and preserved retinal function. In contrast, the treatment of photoreceptors, which are lost in patients at late disease stages, was not therapeutic in *Cln3*$^{\Delta ex7/8}$ mice, underlining the notion that CLN3 disease is primarily a disease of the inner retina with secondary changes in the outer retina. These data indicate that bipolar cells play a central role in this disease and identify this cell type as an important target for ocular AAV-based gene therapies for CLN3 disease.

Introduction

The neuronal ceroid lipofuscinoses (NCLs), also known as Batten disease, is a group of fatal, inherited lysosomal storage disorders (LSDs) predominantly affecting children. The incidence is as high as 1:12,500 in some countries, whilst worldwide it is estimated to be 1:100,000.[1] NCLs are collectively characterized by the gradual accumulation of autofluorescent waste material in the lysosome of neuronal and non-neuronal cells, resulting in severe neuronal and retinal degeneration. Patients present with blindness, seizures, loss of motor and cognitive function, behavioral abnormalities and premature death.[2] NCLs are typically inherited in an autosomal recessive fashion and 13 disease-causing genes were identified that encode soluble or transmembrane proteins, residing mostly in the lysosome or endoplasmatic reticulum (ER).[3]

The most prevalent form of NCL is CLN3 disease, which is caused by mutations in *CLN3*, a gene with elusive function despite more than a decade of research. The ubiquitous CLN3 protein is membrane-bound and primarily present in endosomes and lysosomes.[4] In neurons expression was also reported in axonal extensions and synaptosomes.[5] Classic CLN3 disease presents during early childhood with progressive visual decline from as early as 4 years of age, usually leading to complete loss of vision within less than 2 years. Decline in cognitive abilities, behavioural problems, seizures and motor defects follow. Cardiac abnormalities and death occur in the second and third decade of life.[6] Approximately 85 percent of all CLN3 disease cases are caused by a homozygous 1kb deletion mutation of exon 7 and 8, leading to a truncated protein (for a complete list of mutations see www.ucl.ac.uk/ncl/mutation). Other mutations and compound heterozygosity can have milder clinical manifestation. Of note, adult-onset non-syndromic CLN3 disease with ocular failure devoid of neurological involvement, was found in several unrelated families.[7-9]

Four genetically different *Cln3*-deficient mouse models are available. Unlike most other NCL animal models, all mouse models mimicking CLN3 disease show a mild disease phenotype with a late onset, slow progression and minimally reduced lifespan, hindering the development of treatment.[10] *Cln3*$^{\Delta ex7/8}$ mice, a knock-in mouse line bearing the 1kb deletion mutation commonly found in CLN3 disease patients, have been studied most extensively. The accumulation of lysosomal storage material and neuropathological changes precedes region-specific neuronal loss in these mice, which becomes evident from 12 months.[11,12] A moderate decrease in retinal function with an electronegative response was measured in electroretinography (ERG) recordings,

indicating that the function of inner retinal cells was reduced in *Cln3*$^{\Delta ex7/8}$ mice, whilst the function of the outer retina was not compromised.[12] In line with these findings, the thickness of the inner retina including cells of the inner nuclear layer (INL), ganglion cell layer (GCL) and nerve fiber layer was decreased in another *Cln3*-deficient mouse line. The thickness of the photoreceptor layer and the retinal pigment epithelium (RPE) were not affected.[13] The retinal histology was not assessed in detail in the other mouse models.

There is currently no cure for CLN3 disease. Several therapeutic interventions mostly targeting the brain were tested in preclinical studies using animal models for CLN3 disease or other forms of NCL.[14,15] A handful of treatments were translated to the clinic. Most notably, an enzyme replacement therapy using biweekly intraventricular infusions of tripeptidyl peptidase (TPP1) showed efficacy in CLN2 disease patients [16] and has now been approved by the FDA and EMA. A phase I/II clinical trial using CNS-directed adeno-associated virus (AAV)-mediated gene supplementation therapy is currently ongoing for CLN6 disease patients (NCT02725580). A similar clinical trial was recently started for CLN3 disease (NCT03770572).

As the translation of brain-directed treatments for NCL progresses, the demand for therapies targeting other affected organs like the eye is increasing. This is particularly relevant for transmembrane protein deficiencies of NCL as an effective correction of the ocular phenotype is unlikely upon AAV delivery to the CNS. Recently, we reported that ocular administration of an AAV-based gene therapy rescues the photoreceptor degeneration in *Cln6*-deficient mice, a model for CLN6 disease caused by defects in a membrane-bound protein.[17] Here, we establish that *Cln3*$^{\Delta ex7/8}$ mice show a loss of bipolar cells, interneurons located in the INL of the retina, and confirm the selective dysfunction of the inner retina. We also show that the ocular phenotype can be treated by ubiquitous expression of *CLN3* in the inner retina or cell type-specific expression in bipolar cells of mutant mice. These data provide proof-of-concept supportive of ocular gene therapy targeting the inner retina in CLN3 disease, paving the way towards future clinical translation.

Materials and Methods

Mice

Cln3$^{\Delta ex7/8}$ and C57BL/6J mice were purchased from Harlan Laboratories (UK). All mice were maintained under cyclic light conditions (12h light-dark). Animal experiments were performed in accordance with the ARVO Statement for the Use of Animals in Ophthalmic and Vision Research, and UK Home Office and institutional regulations.

Plasmid construct

Mouse Cln3 (mCln3) cDNA was cloned into a pD10 vector in between the CMV promoter and an internal ribosome entry site (IRES) cassette followed by eGFP. Human CLN3 (hCLN3) cDNA was cloned into a pD10 vector containing the CMV promoter. To drive expression in all ON bipolar cells, hCLN3 cDNA was also cloned into the pAAV vector carrying the 4xGrm6 (4x enhanced mGluR6) promoter kindly provided by Botond Roska (FMI, Basel). pD10.CMV.eGFP and pAAV.Grm6.eGFP plasmids were used to produce control vector.

Production of rAAV

Both recombinant AAV 7m8 and AAV2/8 vector were produced through a triple transient transfection method and purified by affinity-based AVB Sepharose column (GE Healthcare, UK) as described previously.[18] Viral genome titres were determined by quantitative real-time PCR using a probe-based assay annealing to the SV40 poly A tail of the genomic plasmid. Final titres are stated as total viral genome (vg) per eye.

Viral vector administration

Viral vector administration was performed under general anaesthesia using an operating microscope (Carl Zeiss) and a 34 gauge needle (Hamilton). For intravitreal injections, the needle was inserted through the sclera, positioned towards the nasal retina in the vitreal cavity and the viral particles were released. To deliver virus subretinally, the needle was inserted tangentially through the sclera into the subretinal space and the viral particles were released. The needle was withdrawn under great care to support self-sealing. For intravitreal injections a total volume of 1 µl rAAV was administered in early postnatal (P5-P6) mice and for subretinal injection a total volume of 1.5 µl rAAV was administered in juvenile (P14) mice. Left and right eyes were selected for vector administration in an alternating fashion to prevent bias.

Electroretinography (ERG)

ERG recordings were obtained from both eyes in mutant and wild type mice using commercially available equipment (Espion ERG Diagnosys System) as described previously.[19] After dark adaptation overnight, scotopic examinations were performed under single-flash recording using increasing light intensities. Photopic single-flash recordings were obtained following 5 minutes of light adaptation at a background light intensity of 30 cd.s/m^2.

Tissue preparation and immunohistochemistry

Mouse eyes were enucleated and cornea, iris and lens were removed. Eye cups were fixed in 4% PFA for 1-2h, cryoprotected in 20% sucrose and flash frozen in OCT. All eyes were sectioned in a sagittal orientation (12µm), collected on glass slides and stored at -20°C. Prior to use, the slides were briefly thawed, washed in PBS and blocking buffer was employed containing 5% NGS, 1% BSA and 0.1% Triton-X100. The samples were incubated in primary antibody diluted in blocking buffer at 4°C overnight (anti-PKCα 1:500 (Sigma-Aldrich), anti-GFAP 1:300 (Merck Chemicals), anti-eGFP 1:300 (Life Technologies), anti-Calbindin 1:100 (Abcam), anti-cone-arrestin 1:300 (Millipore), anti-CRALBP 1:300 (Abcam)). Sections were washed in PBS and incubated in secondary antibody diluted in blocking buffer (Alexa Fluor® 546 anti-mouse IgG 1:500, Alexa Fluor® 633 anti-rat IgG 1:500 (both Life Technologies)). Sections were washed in PBS, incubated with 600nM DAPI for 5 minutes and mounted in DAKO mounting media. The slides were stored in the dark at 4°C until imaging by confocal microscopy (Leica DM5500Q).

Quantification of retinal cross sections

For quantifications of rod bipolar and horizontal cells, merged confocal images (consisting of 12-13 z-stacks) of the same size (275µm x 275µm) were taken from the superior and inferior midcentral retina of three sagittal cross sections (in total six images per eye). The number of PKCα-positive and Calbindin-positive cells were counted in all images and averaged for each eye. Researchers performing counts were masked to the genotype of the animals and treatment received.

Statistical analysis

Data are represented as means ± SD (standard deviation) with the appropriate *n* (number of samples) values as indicated. Statistical analyses were performed using GraphPad Prism 5 for Windows. The appropriate tests and p values are provided.

Results

$Cln3^{\Delta ex7/8}$ *mice have reduced inner retinal function accompanied by the loss of rod bipolar cells*

Cln3$^{\Delta ex7/8}$ mice were reported to have a mild decline in retinal function, yet no morphological phenotype of the retina was described.[12] To confirm the retinal phenotype and to establish parameters to measure the therapeutic outcome, we performed ERG recordings in *Cln3*$^{\Delta ex7/8}$ mice and age-matched wild type controls over time. In agreement with previous work, at 12 months we observed a moderate but significant reduction in the size of the scotopic and photopic b-wave amplitudes, indicative of a decline in rod- and cone-mediated inner retinal function. At 15 months, this decrease progressed slightly, whilst the scotopic and photopic a-wave amplitudes remained unchanged (see figure S1). A table with an overview of the scotopic and photopic b-wave amplitudes at 12 and 15 months can be found in table S1 and S2 (see supplementary information).

We investigated the retinal morphology in mutant mice and stained for PKCα, a marker for rod bipolar cells, which are retinal interneurons of the INL that predominantly contribute to the scotopic b-wave amplitude.[20] Rod bipolar cells receive direct input from rod photoreceptors and subsequently transmit signals to retinal ganglion cells. In 12-months-old mutants the mid-retina appeared to have fewer PKCα-positive cells. At 15 months the lack of rod bipolar cells became more apparent in the mid-retina and was very obvious in the periphery of the retina when compared with age-matched controls (figure 1A-B). To assess the loss of bipolar cells, we counted the number of PKCα-positive cells in the mid-retina and found a significantly reduced number of cells in mutants compared with wild type controls at 15 months ($p = 0.0079$) (figure 1C). In contrast, quantification of Calbindin-positive horizontal cells, a cell type that together with ON bipolar cells forms the post-synaptic entity of the photoreceptor ribbon synapses, did not reveal a significant difference between mutant and wild type retinas (figure 1D-E). We also stained for glial fibrillary acidic protein (GFAP), a common marker for astrocytes and reactive gliosis, that is up-regulated in retinas of other NCL models.[17,21] At both timepoints we did not observe a severe increase in GFAP staining in the mid-retina. A mild GFAP up-regulation in Mueller glia cells, spanning the width of the retina, and in astrocytes, located in the nerve fiber layer of the retina, was present in the mid- and peripheral retina in mutants at 15 months (figure 1B). Immunohistochemical staining for cellular retinalaldehyde binding protein (CRLABP)

showed a similar pattern of Mueller glia cell bodies and processes in mutant and wild type retinas, indicating that there was no obvious cell loss in *Cln3*-deficient mice (figure 1F). In line with normal photoreceptor function demonstrated by unaffected scotopic and photopic a-wave amplitudes, the thickness of the outer nuclear layer (ONL) and the number of cone-arrestin (CAR) -positive cells did not appear to be noticeably decreased in $Cln3^{\Delta ex7/8}$ retinas (figure S1A, S1B, 1D).

7m8-mediated delivery of mouse Cln3 to the inner retina rescues retinal phenotype of* Cln3$^{\Delta ex7/8}$ *mice.

Due to the lack of a good anti-Cln3 antibody and the low protein abundance, we were not able to assess the endogenous *Cln3* expression in the different cell types of the retina. In $Cln3^{lacZ/lacZ}$ mice, a knock-in reporter mouse line harboring b-galactosidase in the *Cln3* locus, the expression of the lacZ reporter was first detected in bipolar cells and later became apparent in photoreceptors.[22] Microarray and RNAseq analyses found *Cln3* expression in bipolar cells, photoreceptors and microglia in the adult mouse and human retina (https://www.fmi.ch/roska.data/index.php).[23,24] Because $Cln3^{\Delta ex7/8}$ mice showed an inner retinal dysfunction and a loss of bipolar cells, we focused on developing an AAV-based gene therapy using AAV 7m8, a variant of AAV2/2,[25] engineered to target the inner retina and able to transduce bipolar cells across the width of the retina. We performed intravitreal injections with 7m8 carrying the CMV promoter, the mouse *Cln3* (mCln3) transgene and an internal ribosomal entry site (IRES) cassette followed by eGFP. We administered the vector in postnatal day (P) 5-6 $Cln3^{\Delta ex7/8}$ mice at a high dose of $1x10^{10}$ total viral genome (vg) per eye or a low dose of $1x10^{9}$ vg per eye. Contralateral eyes received injections with 7m8.CMV.eGFP at $1x10^{10}$ vg or were left uninjected as controls.

At 12 months, the scotopic and photopic b-waves were significantly higher at a light intensity of 1 cd.s/m^2 in *mCln3*-treated than in untreated or eGFP-treated mutant eyes with a larger effect in eyes that received the high dose vector. The size of the b-wave amplitudes decreased in untreated and eGFP-treated eyes at 15 months, whilst the amplitudes were maintained in *Cln3*-treated eyes in a dose-dependent manner, indicating that the therapeutic effect was sustained over time (figure 2A, S2A, table S1, S2). Representative scotopic ERG traces of a mutant mouse that received injections with the therapeutic vector at high dose in one eye (red traces) and no treatment in the contralateral eye (black traces) are shown in figure 2B. In the absence of an antibody

detecting Cln3, we performed immunostainings with an anti-eGFP antibody and observed a low fluorescent signal in various cell types, including photoreceptors and bipolar cells, in treated retinas at 15 months. The low expression level of eGFP can most likely be explained by the presence of the IRES cassette. Comparison with 7m8.CMV.eGFP-treated retinas demonstrate the widespread transduction of cells throughout all layers of the retina, consistent with previous reports.[17,25] Immunostaining for PKCα revealed that there was significantly a higher number of rod bipolar cells in the mid-retina of mutants treated with high dose 7m8.CMV.mCln3-ires-eGFP than eGFP-treated or untreated mutant retinas (figure 2C, 2D). Similar to the findings in the mid-retina, the therapeutic effect on the survival of rod bipolar cells was also apparent in the peripheral retina of treated *Cln3*$^{\Delta ex7/8}$ mice and representative images are shown in figure S2B.

Intravitreal injections of 7m8 lead to the transduction of approximately 25 percent of photoreceptors in mouse retinas.[17] To exclude that transgene expression in photoreceptors contributed to the therapeutic effect, we also performed subretinal injections with AAV2/8, an AAV serotype commonly used to target photoreceptors and RPE.[26] *Cln3*-deficient pups received injections in one eye with a 1.5x10^{10} vg AAV2/8, harbouring mCln3-ires-eGFP under the control of the CMV promoter. Contralateral mutant eyes received injections with AAV2/8.CMV.eGFP or remained uninjected. At 12 and 15 months, no preservation of the scotopic b-wave amplitudes were detected in *Cln3*-treated compared with eGFP-treated or uninjected eyes, indicating that transgene expression in photoreceptors was not therapeutic in *Cln3*$^{\Delta ex7/8}$ mice (figure 2A, S2A, table S1, S2). Histological assessment of AAV2/8.mCln3-treated retinas at 15 months confirmed transgene expression in photoreceptors and the loss of PKCα-positive bipolar cells, comparable with untreated retinas (figure S2B, 2C).

Overexpression of human CLN3 is therapeutic in Cln3$^{\Delta ex7-8}$ *mice*

To investigate whether the delivery of the human transgene, which shares over 80% sequence homology with the mouse gene,[27] corrected the retinal phenotype, we also produced 7m8 carrying the CMV promoter and the human *CLN3* gene (hCLN3). No ires cassette or fluorescent reporter was included because poor eGFP expression levels were observed in retinas treated with 7m8.CMV.mCln3-ires-eGFP. *Cln3*-deficient pups received intravitreal injections with 7m8.CMV.hCLN3 at 1x10^{10} vg and ERG recordings were performed to measure retinal function. At 12 months, the scotopic and

photopic b-waves were significantly higher in treated compared with untreated mutant eyes and they remained higher than untreated eyes at 15 months (figure 3A, S3A, table S1, S2). Figure 3B shows example traces of scotopic ERG recordings from a 15-months old *Cln3*$^{\Delta ex7/8}$ mouse with a treated (red traces) and an untreated eye (black traces). Histological assessment indicated that there were more PKCα-positive bipolar cells in treated than untreated mutant retinas at 15 months in the mid-retina (figure 3C) and the peripheral retina (figure S3C). Quantification of the cell numbers established that a significantly higher number of rod bipolar cells was present in mutants following the treatment (figure 3D).

Bipolar cell specific expression of human CLN3 rescues retinal phenotype of* Cln3-*deficient mice

Untreated *Cln3*$^{\Delta ex7/8}$ mice show a significant decline in the ERG b-waves and a loss of bipolar cells. To assess whether *CLN3* overexpression in bipolar cells was sufficient to treat the ocular phenotype in mutant mice, a 7m8 vector was produced that carried *CLN3* under the control of the Grm6 promoter, predominantly driving expression in rod bipolar cells.[28] P5-P6 mutant mice were injected intravitreally with 7m8.Grm6.hCLN3 at either 1x10^{9} vg or 1x10^{10} vg. Contralateral eyes were not injected to provide internal age-matched controls.

ERG recordings at 12 and 15 months demonstrated that the scotopic b-waves were higher in treated mutant eyes in a dose-dependent manner at the light intensity of 1cd.s/m^{2}. Statistical significance was reached at 15 months in eyes that received high titre 7m8.Grm6.hCLN3 compared with untreated mutant eyes (figure 4A, table S1). The overlay of the scotopic ERG traces underlines the therapeutic effect in a high titre treated eye (red traces) compared with an untreated contralateral eye (black traces) across a range of light intensities (figure 4B). The analysis of the photopic b-waves amplitudes did not show a significant difference between Grm6.hCLN3-treated and untreated eyes (figure S3B, table S2) unlike CMV.hCLN3-treated mutant eyes (figure S3A, table S2), which may be due to a combination of the low transduction efficiency of cone bipolar cells following the administration of 7m8[29] and the lower transgene expression levels in cone bipolar cells. In line with the scotopic ERG recordings, a significantly higher number of PKCα-positive bipolar cells was detected in eyes that received low and high titre 7m8.Grm6.hCLN3 than untreated mutant eyes (figure 4C-D, S3C).

Discussion

The development of therapies for NCLs targeting the brain has seen big advances over the last decade. CNS-directed enzyme replacement therapy received FDA and EMA approval for CLN2 disease and two phase I/II gene therapy clinical trials, one for CLN6 and one CLN3 disease patients, are currently ongoing (NCT02725580) (NCT03770572). Although the studies are encouraging to combat the neurodegeneration, these therapeutic interventions are unlikely to treat the retinal degeneration and NCL patients will most likely continue to go blind. To address this need for ocular treatments, we studied the retinal phenotype of *Cln3*$^{\Delta ex7/8}$ mice, a model for CLN3 disease, and found that retinal function can be maintained long-term by pre-symptomatically delivered ocular gene therapy. We confirm that *Cln3*-deficient mice suffer from a late and mildly progressing decline of inner retinal function and we discovered a significant decrease in rod bipolar cell counts, especially evident in the peripheral retina. Ubiquitous AAV-mediated *CLN3* expression in cells of the inner retina or bipolar-specific expression successfully prevented the loss of retinal function and bipolar cells in mutant mice, establishing the inner retina as the prime target for ocular gene therapy in CLN3 disease.

Inherited retinopathies due to gene defects in photoreceptors and the RPE are a common cause of blindness. Several ocular gene therapies targeting the outer retina have been translated into the clinic including Leber congenital amaurosis,[30-33] retinitis pigmentosa[34] and achromatopsia.[35] Retinal diseases caused by mutated genes in cells of the inner retina, leading to loss of inner retinal function, are rare. Electronegative ERG responses characterized by a more pronounced loss of the b- than the a-wave were described in early symptomatic CLN3 disease patients preceding the complete loss of retinal function at advanced disease stages.[36-38] Post-mortem tissue of patients revealed gross disturbances of the retinal morphology, severe thinning of all retinal layers and a complete lack of photoreceptors in the mid and central retina.[39] As *CLN3* was reported to be expressed in photoreceptors in mice [22,23] and humans [24] and photoreceptors are absent at disease end stage, it was suggested that gene supplementation therapy targeting the outer retina by subretinal injections could be an effective strategy to treat the ocular failure in CLN3 disease.[40] Here, we show that the AAV2/8-mediated overexpression of *Cln3* in photoreceptors is not therapeutic in *Cln3*$^{\Delta ex7/8}$ mice and that

instead the transduction of inner retinal cells, especially bipolar cells, is crucial for successful ocular *CLN3* gene therapy. Of note is, that the current CNS-directed gene therapy clinical trial for CLN3 disease uses AAV2/9, an AAV serotype that similar to AAV2/8 transduces photoreceptors and the RPE well, yet does not target cells in the inner retina [41]. In line with other reports,[12,13] we did not observed any reduction in photoreceptor function or obvious photoreceptor death in *Cln3*-deficient mice. Why mutant mice fail to reproduce the secondary loss of photoreceptors observed in patients remains unclear. It could be speculated that the photoreceptor loss in (end-stage) patients is entirely secondary to bipolar cell defect (note that such a mechanism is also present in *Cln6*^{nclf} mice, where treatment of bipolar cells rescued the loss of photoreceptor cells[17]). As the degeneration in *Cln3*$^{\Delta ex7/8}$ mice is slow, it could be that there is not enough time for the bipolar cells death to substantially affect the ONL. Why the degeneration is so slow in mice is not clear, but this observation is not uncommon in ophthalmic research. For example, the *rd1* mouse, a model that carries a mutation in the photoreceptor cGMP phosphodiesterase 6b (*Pde6b*) gene, shows a much faster disease progression than patients[42] and the *RPGR* mouse, a model that carries a mutation in the retinitis pigmentosa GTPase regulator gene, shows a slower degeneration than patients.[43] Whilst it cannot be fully excluded that there is a primary photoreceptor loss in CLN3 disease patients that is not replicated in the mice, which would not be treated with our approach, the electronegative ERG in patients together with our study data strongly suggests that bipolar cell loss in patients is very likely a direct effect and that gene transfer to these cells is a prerequisite for successful treatment in patients.

Recently we reported another ocular gene therapy targeting the inner retina in *Cln6*^{nclf} mice, a model for variant late-infantile CLN6 disease. Although *Cln6*-deficient mice predominantly lose photoreceptors and bipolar cells only die at late disease stages, 7m8-mediated gene supplementation of bipolar cells prevented the photoreceptor degeneration in these mice.[17] Similar to *CLN3, CLN6* is expressed in bipolar and photoreceptor cells,[17,23] encoding a membrane-bound protein of unknown function. Despite these similarities, CLN3 and CLN6 are located in different cell organelles and have been implicated in different cell functions.[3] The retinal disease mechanism in CLN3 and CLN6 disease is not understood, however our studies demonstrate that in both forms of the disease cells in the inner retina and in particular bipolar cells play a central role. We therefore recommend that efforts to unravel the function of retinal

degeneration associated genes and their disease mechanisms, such as *in vitro* disease modeling using iPS-derived retinal cultures, should not be limited to the study of photoreceptors but should also focus on cells of the inner retina to uncover relevant disease features.

Intravitreal administration of 7m8 and other AAVs including AAV2/2 and tyrosine-mutated AAV2/2 transduce bipolar cells and other cells of the inner retina well in mice. However, the transduction efficiency of these vectors is lower in larger animals due to the substantially thicker inner limiting membrane (ILM) and the vitreous humor, both acting as physical barriers for AAVs.[25,44] Surgical peeling of the ILM and vitrectomy to remove vitreous prior to intravitreal injections resulted in a localized, enhanced retinal transduction in non-human primate (NHP) retinas.[45,46] However, it remains to be established if ILM removal in diseased eyes in combination with intravitreal AAV injections pose additional inflammatory challenges that would need to be addressed in the clinic. Optimization of bipolar cell transduction from the subretinal space has been explored and the synthetic AAV8BP2 was shown to target bipolar cells in mice,[28] yet the transduction efficiency of the INL appeared to be low in NHPs.[47] It is important to point out that in these NHP studies ubiquitous promoters are commonly used, driving expression in all cell types of the INL, which makes it difficult to specifically identify bipolar cells and estimate their transduction efficiency. Large animal studies using bipolar cell type specific promoters could facilitate the search and optimization of AAVs targeting bipolar cells. Whilst there is currently no AAV available to achieve widespread expression in the INL of large animals, intravitreal administration of 7m8 in NHPs results in a good transduction of the fovea and parafovea,[25] a region that was reported to be spared or affected late in CLN3 disease patients.[8] Although 7m8 may not be the ideal candidate vector to achieve an extensive transduction of the inner retina and the development of more efficacious vectors should be considered, the 7m8 vector could provide a successful strategy to maintain central vision and thereby could improve quality of life of patients substantially.

Acknowledgments

This project was supported by the Batten Disease Family Association, charity No 1084908, the European Union's Horizon 2020 research and innovation programme (Grant No 66691), RP Fighting Blindness (Grant GR576), and Medical Research Council (Grant No MR/R025134/1). RRA is partially supported by the NIHR Biomedical Research Centre at Moorfields Eye Hospital and the UCL Institute of Ophthalmology.

Author disclosure statement

The authors do not declare any conflicts of interest.

References:

1 Mole S, Williams R, Goebel H. *The Neuronal Ceroid Lipofuscinoses (Batten Disease)*. OUP Oxford, 2011

2 Schulz A, Kohlschütter A, Mink J, Simonati A, Williams R. NCL diseases - clinical perspectives. *Biochim Biophys Acta* 2013; **1832**: 1801–1806.

3 Kollmann K, Uusi-Rauva K, Scifo E, Tyynelä J, Jalanko A, Braulke T. Cell biology and function of neuronal ceroid lipofuscinosis-related proteins. *Biochim Biophys Acta* 2013; **1832**: 1866–1881.

4 Kyttälä A, Ihrke G, Vesa J, Schell MJ, Luzio JP. Two Motifs Target Batten Disease Protein CLN3 to Lysosomes in Transfected Nonneuronal and Neuronal Cells. *Molecular Biology of the Cell* 2004; **15**: 1313.

5 Luiro K, Kopra O, Lehtovirta M, Jalanko A. CLN3 protein is targeted to neuronal synapses but excluded from synaptic vesicles: new clues to Batten disease. *Human Molecular Genetics* 2001; **10**: 2123–2131.

6 Ostergaard JR, Rasmussen TB, Mølgaard H. Cardiac involvement in juvenile neuronal ceroid lipofuscinosis (Batten disease). *Neurology* 2011; **76**: 1245–1251.

7 Wang F, Wang H, Tuan H-F, Nguyen DH, Sun V, Keser V *et al.* Next generation sequencing-based molecular diagnosis of retinitis pigmentosa: identification of a novel genotype-phenotype correlation and clinical refinements. *Hum Genet* 2014; **133**: 331–345.

8 Ku CA, Hull S, Arno G, Vincent A, Carss K, Kayton R *et al.* Detailed Clinical Phenotype and Molecular Genetic Findings in CLN3-Associated Isolated Retinal Degeneration. *JAMA Ophthalmology* 2017; **135**: 749.

9 Chen FK, Zhang X, Eintracht J, Zhang D, Arunachalam S, Thompson JA *et al.* Clinical and molecular characterization of non-syndromic retinal dystrophy due to c.175G>A mutation in ceroid lipofuscinosis neuronal 3 (CLN3). *Doc Ophthalmol* 2018; **138**: 55–70.

10 Bond M, Holthaus S-MK, Tammen I, Tear G, Russell C. Use of model organisms for the study of neuronal ceroid lipofuscinosis. *Biochim Biophys Acta* 2013; **1832**: 1842–1865.

11 Cotman SL, Vrbanac V, Lebel LA, Lee RL, Johnson KA, Donahue LR *et al.* Cln3(Deltaex7/8) knock-in mice with the common JNCL mutation exhibit progressive neurologic disease that begins before birth. *Human Molecular Genetics* 2002; **11**: 2709–2721.

12 Staropoli JF, Haliw L, Biswas S, Garrett L, Hölter SM, Becker L *et al.* Large-Scale Phenotyping of an Accurate Genetic Mouse Model of JNCL Identifies Novel Early Pathology Outside the Central Nervous System. *PLoS ONE* 2012; **7**: e38310.

13 Groh J, Stadler D, Buttmann M, Martini R. Non-invasive assessment of retinal alterations in mouse models of infantile and juvenile neuronal ceroid lipofuscinosis by spectral domain optical coherence tomography. *Acta Neuropathol Commun* 2014; **2**: 54.

14 Biffi A. Gene therapy for lysosomal storage disorders: a good start. *Human Molecular Genetics* 2016; **25**: R65–R75.

15 Kleine Holthaus S-M, Smith AJ, Mole SE, Ali RR. Gene Therapy Approaches to Treat the Neurodegeneration and Visual Failure in Neuronal Ceroid Lipofuscinoses. In: *link.springer.com*. Springer International Publishing: Cham, 2018, pp 91–99.

16 Schulz A, Ajayi T, Specchio N, de Los Reyes E, Gissen P, Ballon D *et al.* Study of Intraventricular Cerliponase Alfa for CLN2 Disease. *N Engl J Med* 2018; **378**: 1898–1907.

17 Kleine Holthaus S-M, Ribeiro J, Abelleira Hervas L, Pearson RA, Duran Y, Georgiadis A *et al.* Prevention of Photoreceptor Cell Loss in a Cln6nclf Mouse Model of Batten Disease Requires CLN6 Gene Transfer to Bipolar Cells. *Molecular Therapy* 2018; **26**: 1343–1353.

18 Davidoff AM, Ng CYC, Sleep S, Gray J, Azam S, Zhao Y *et al.* Purification of recombinant adeno-associated virus type 8 vectors by ion exchange chromatography generates clinical grade vector stock. *J Virol Methods* 2004; **121**: 209–215.

19 Nishiguchi KM, Carvalho LS, Rizzi M, Powell K, Holthaus S-MK, Azam SA *et al.* Gene therapy restores vision in rd1 mice after removal of a confounding mutation in Gpr179. *Nat Comms* 2015; **6**: 6006.

20 Stockton RA, Slaughter MM. B-wave of the electroretinogram. A reflection of ON bipolar cell activity. *J Gen Physiol* 1989; **93**: 101–122.

21 Jankowiak W, Brandenstein L, Dulz S, Hagel C, Storch S, Bartsch U. Retinal Degeneration in Mice Deficient in the Lysosomal Membrane Protein CLN7. *Invest Ophthalmol Vis Sci* 2016; **57**: 4989.

22 Ding S-L, Tecedor L, Stein CS, Davidson BL. A knock-in reporter mouse model for Batten disease reveals predominant expression of Cln3 in visual, limbic and subcortical motor structures. *Neurobiol Dis* 2011; **41**: 237–248.

23 Siegert S, Cabuy E, Scherf BG, Kohler H, Panda S, Le Y-Z *et al.* Transcriptional code and disease map for adult retinal cell types. *Nat Neurosci* 2012; **15**: 487–495.

24 Lukowski SW, Lo CY, Sharov AA, Nguyen Q, Fang L, Hung SS *et al.* A single-cell transcriptome atlas of the adult human retina. *Embo J* 2019; **38**: 2738.

25 Dalkara D, Byrne LC, Klimczak RR, Visel M, Yin L, Merigan WH *et al.* In Vivo-Directed Evolution of a New Adeno-Associated Virus for Therapeutic

Outer Retinal Gene Delivery from the Vitreous. *Science Translational Medicine* 2013; **5**: 189ra76–189ra76.

26 Ivana Trapani, Pasqualina Colella, Sommella A, Iodice C, Cesi G, de Simone S *et al.* Effective delivery of large genes to the retina by dual AAV vectors. *EMBO Molecular Medicine* 2014; **6**: 194.

27 Taschner P, de Vos N, Breuning M. Cross-Species Homology of the CLN3 Gene. *Neuropediatrics* 1997; **28**: 18–20.

28 Cronin T, Vandenberghe LH, Hantz P, Juttner J, Reimann A, Kacso AE *et al.* Efficient transduction and optogenetic stimulation of retinal bipolar cells by a synthetic adeno-associated virus capsid and promoter. *EMBO Molecular Medicine* 2014; **6**: 1175–1190.

29 van Wyk M, Hulliger EC, Girod L, Ebneter A, Kleinlogel S. Present Molecular Limitations of ON-Bipolar Cell Targeted Gene Therapy. *Front Neurosci* 2017; **11**: 11372.

30 Bainbridge JWB, Mehat MS, Sundaram V, Robbie SJ, Barker SE, Ripamonti C *et al.* Long-Term Effect of Gene Therapy on Leber's Congenital Amaurosis. *N Engl J Med* 2015; **372**: 1887–1897.

31 Weleber RG, Pennesi ME, Wilson D, Kaushal S, Erker L, Jensen L *et al.* Results at 2 Years after Gene Therapy for RPE65-Deficient Leber Congenital Amaurosis and Severe Early-Childhood–Onset Retinal Dystrophy. *Ophthalmology* 2016; **123**: 1606–1620.

32 Guylène Le Meur, Lebranchu P, Billaud F, Adjali O, Schmitt S *et al*. Safety and Long-Term Efficacy of AAV4 Gene Therapy in Patients with RPE65 Leber Congenital Amaurosis. *Molecular Therapy* 2018; **26**: 256–268.

33 Maguire AM, Russell S, Wellman JA, Chung DC, Yu Z-F, Tillman A *et al.* Efficacy, Safety, and Durability of Voretigene Neparvovec-rzyl in RPE65 Mutation–Associated Inherited Retinal Dystrophy. *Ophthalmology* 2019; **126**: 1273–1285.

34 Ghazi NG, Abboud EB, Nowilaty SR, Alkuraya H, Alhommadi A, Cai H *et al.* Treatment of retinitis pigmentosa due to MERTK mutations by ocular subretinal injection of adeno-associated virus gene vector: results of a phase I trial. *Hum Genet* 2016; **135**: 327–343.

35 Kahle N, Peters T, Zobor D, Kuehlewein L, Kohl S, Zhour A *et al.* Development of Methodology and Study Protocol: Safety and Efficacy of a Single Subretinal Injection of rAAV.hCNGA3 in Patients with CNGA3-Linked Achromatopsia Investigated in an Exploratory Dose-Escalation Trial. *Human Gene Therapy Clinical Development* 2018.

36 Weleber RG. The dystrophic retina in multisystem disorders: the electroretinogram in neuronal ceroid lipofuscinoses. *Eye (Lond)* 1998; **12 (Pt 3b)**: 580–590.

37 Eksandh LB, Ponjavic VB, Munroe PB, Eiberg HE, Uvebrant PE, Ehinger BE *et al.* Full-field ERG in patients with Batten/Spielmeyer-Vogt disease caused by mutations in the CLN3 gene. *Ophthalmic Genet* 2000; **21**: 69–77.

38 Collins J, Holder GE, Herbert H, Adams GGW. Batten disease: features to facilitate early diagnosis. *The British Journal of Ophthalmology* 2006; **90**: 1119–1124.

39 Bensaoula T, Shibuya H, Katz ML, Smith JE, Johnson GS, John SK *et al.* Histopathologic and immunocytochemical analysis of the retina and ocular tissues in Batten disease. *Ophthalmology* 2000; **107**: 1746–1753.

40 Wiley LA, Burnight ER, Drack AV, Banach BB, Ochoa D, Cranston CM *et al.* Using Patient-Specific Induced Pluripotent Stem Cells and Wild-Type Mice to Develop a Gene Augmentation-Based Strategy to Treat CLN3-Associated Retinal Degeneration. *Human Gene Therapy* 2016; **27**: 835–846.

41 Vandenberghe LH, Bell P, Maguire AM, Xiao R, Hopkins TB, Grant R *et al.* AAV9 targets cone photoreceptors in the nonhuman primate retina. *PLoS ONE* 2013; **8**: e53463.

42 Bowes C, Li T, Danciger M, Baxter LC, Applebury ML, Farber DB. Retinal degeneration in the rd mouse is caused by a defect in the β subunit of rod cGMP-phosphodiesterase. *Nature* 1990; **347**: 677–680.

43 Hong DH. A retinitis pigmentosa GTPase regulator (RPGR)- deficient mouse model for X-linked retinitis pigmentosa (RP3). *Proceedings of the National Academy of Sciences* 2000; **97**: 3649–3654.

44 Mowat FM, Gornik KR, Dinculescu A, Boye SL, Hauswirth WW, Petersen-Jones SM *et al.* Tyrosine capsid-mutant AAV vectors for gene delivery to the canine retina from a subretinal or intravitreal approach. *Gene Ther* 2013; **21**: 96–105.

45 Takahashi K, Igarashi T, Miyake K, Kobayashi M, Yaguchi C, Iijima O *et al.* Improved Intravitreal AAV-Mediated Inner Retinal Gene Transduction after Surgical Internal Limiting Membrane Peeling in Cynomolgus Monkeys. *Molecular Therapy* 2017; **25**: 296–302.

46 Teo KYC, Lee SY, Barathi AV, Tun SBB, Tan L, Constable IJ. Surgical Removal of Internal Limiting Membrane and Layering of AAV Vector on the Retina Under Air Enhances Gene Transfection in a Nonhuman Primate. *Invest Ophthalmol Vis Sci* 2018; **59**: 3574–3583.

47 Ramachandran PS, Lee V, Wei Z, Song JY, Casal G, Cronin T *et al.* Evaluation of Dose and Safety of AAV7m8 and AAV8BP2 in the Non-Human Primate Retina. *Human Gene Therapy* 2017; **28**: 154–167.

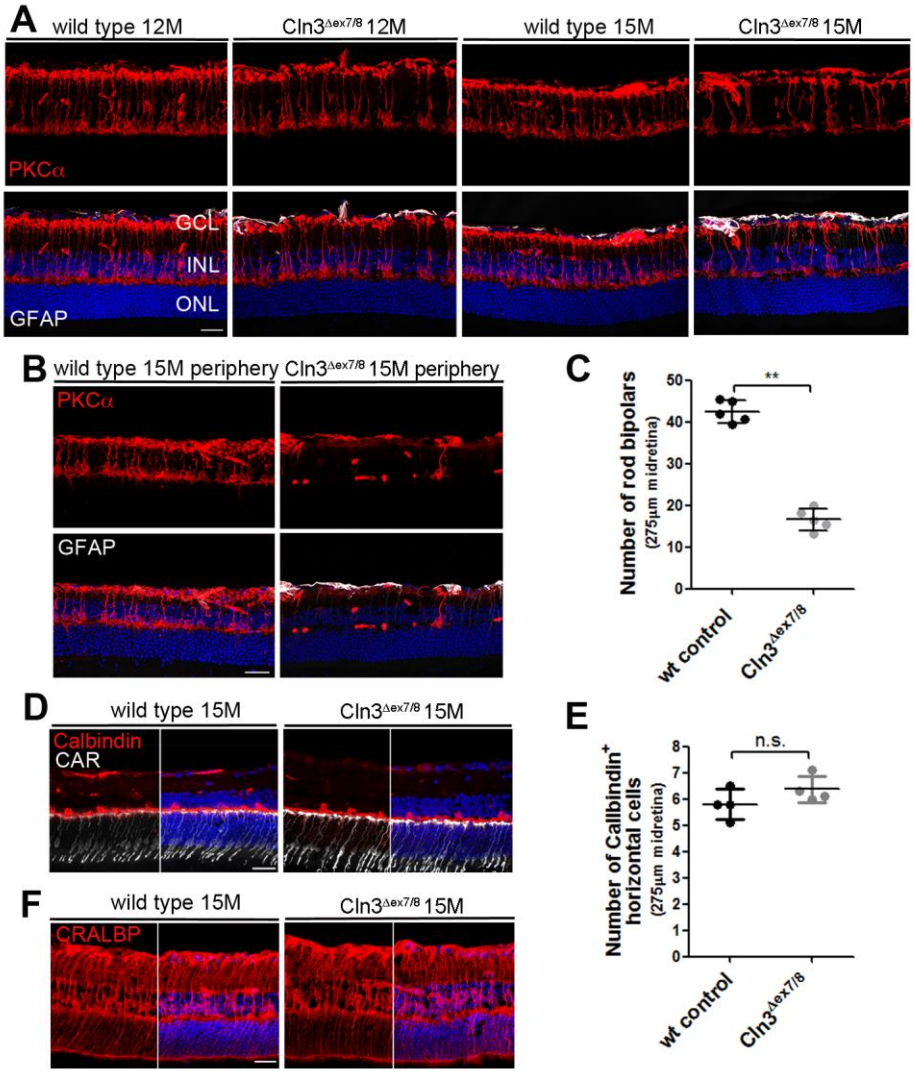

Figure 1: *Cln3*$^{\Delta ex7/8}$ mice show a progressive loss of rod bipolar cells

(A) Representative confocal images of the mid-retina from *Cln3*$^{\Delta ex7/8}$ and wild type mice immunostained with antibodies against PKCα and GFAP. At 12 months fewer PKCα-positive cells were detected in mutant than wild type retinas, which progressed to an obvious loss of cells at 15 months. GFAP staining did not appear to be elevated. **(B)** PKCα staining revealed a pronounced lack of rod bipolar cells in the periphery of the retina. **(C)** Quantification of the number of PKCα-positive rod bipolar cells in the mid-retina of mutant and wild type retinas at 15 months. Wild type and *Cln3*$^{\Delta ex7/8}$: n = 5 eyes. Data are presented as means ± SD and analysed by a non-parametric Mann-Whitney test (**p = 0.0079). **(D, F)** Representative images of 15 months-old mutant and wild type midretina immunostained for Calbindin, cone-arrestin (CAR) and CRLABP. No obvious loss of horizontal, cone-photoreceptor and Mueller glia cells was observed. **(E)** Quantification of the number of Calbindin-positive cells in the INL did not reveal any significant difference between mutant and wild type retinas at 15 months. Wild type and *Cln3*$^{\Delta ex7/8}$: n = 4 eyes. Data are presented as means ± SD. Scale bar: 25µm. GCL = ganglion cell layer, INL = inner nuclear layer, ONL = outer nuclear layer.

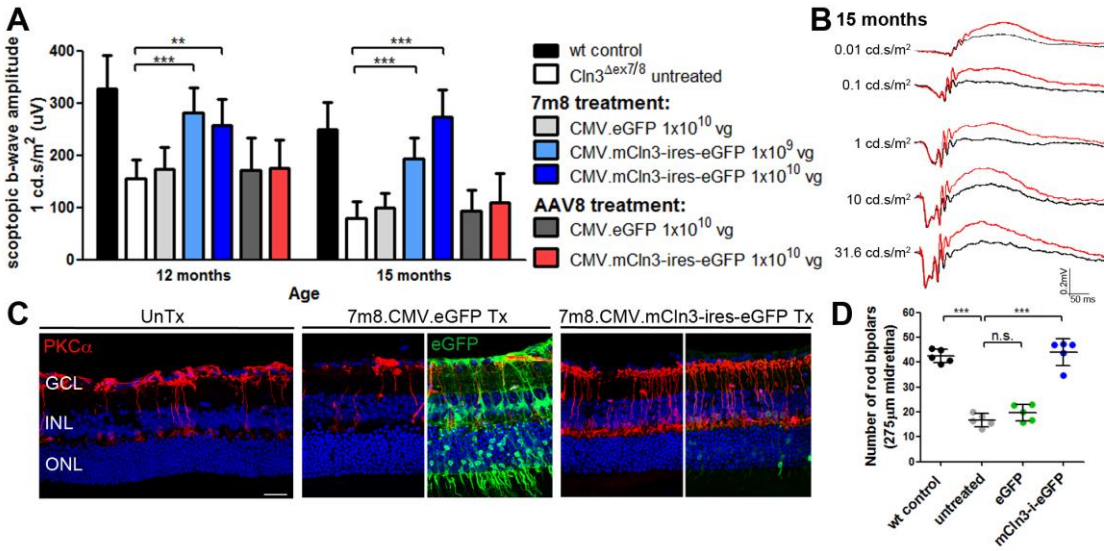

Figure 2: Intravitreally delivered 7m8.CMV.mCln3-ires-eGFP treats the ocular phenotype in *Cln3*-deficient mice

(A) Scotopic ERG b-wave recordings of *Cln3*$^{\Delta ex7/8}$ mice at a light intensity of 1 cd.s/m^2 following the intravitreal and subretinal administration of 7m8.CMV.mCln3-ires-eGFP and AAV8.CMV.mCln3-ires-eGFP, respectively. Wild type: n = 7-8 eyes, *Cln3*$^{\Delta ex7/8}$ untreated: n = 19 eyes, 7m8.CMV.eGFP: n = 5-6 eyes, 7m8.CMV.mCln3-ires-eGFP 1 x 10^9 vg: n = 5-6 eyes, 7m8.CMV.mCln3-ires-eGFP 1 x 10^{10} vg: n = 5 eyes, AAV8.CMV.eGFP: n = 3 eyes, AAV8.CMV.mCln3-ires-eGFP: n = 4 eyes. Wild type recordings from figure 1 were added as a reference. **(B)** Scotopic ERG traces of a mutant mouse treated with 1 x 10^{10} vg 7m8.CMV.mCln3-ires-eGFP in one eye (red). The contralateral eye did not receive treatment (black). **(C)** PKCα staining on untreated, 7m8.CMV.eGFP- and 7m8.CMV.mCln3-ires-eGFP-treated mid-retinas at 15 months. eGFP-staining was performed to visualise mCln3-ires-eGFP transduced cells. **(D)** Quantification of number of rod bipolar cells in the mid-retina of mutant mice treated with 7m8. Data are presented as means ± SD and analysed by **(A)** two-way ANOVA with Bonferroni or **(D)** one-way ANOVA with Kruskall-Wallis test (**p < 0.01, ***p < 0.001). Scale bar: 25µm.

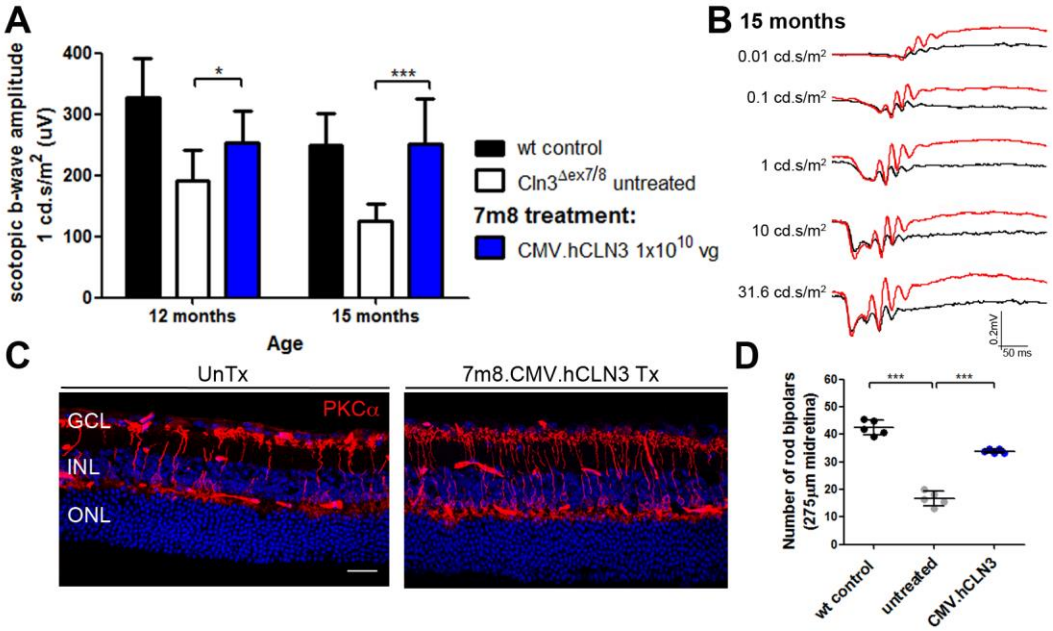

Figure 3: Intravitreal administration of 7m8.CMV.hCLN3 prevents the loss of retinal function and bipolar cells in *Cln3$^{\Delta ex7/8}$* mice

(A) Scotopic ERG b-wave amplitudes of 7m8.CMV.hCLN3-treated mutant mice. Wild type: n = 7-8 eyes, *Cln3$^{\Delta ex7/8}$*: n = 8 eyes, 7m8.CMV.hCLN3: n = 10 eyes. Wild type recordings from figure 1 were added as a reference. **(B)** Scotopic ERG traces of a *Cln3$^{\Delta ex7/8}$* mouse that received treatment in one eye (red) and no treatment in the contralateral eye (black). **(C)** Confocal images of the mid-retina from untreated and 7m8.CMV.hCLN3-treated eyes stained for PKCα at 15 months. **(D)** Counts of PKCα-positive cells in the mid-retina at 15 months. Data are presented as means ± SD and analysed by **(A)** two-way ANOVA with Bonferroni test and **(D)** one-way ANOVA with Kruskal Wallis test (*$p < 0.05$, ***$p < 0.001$). Scale bar: 25µm.

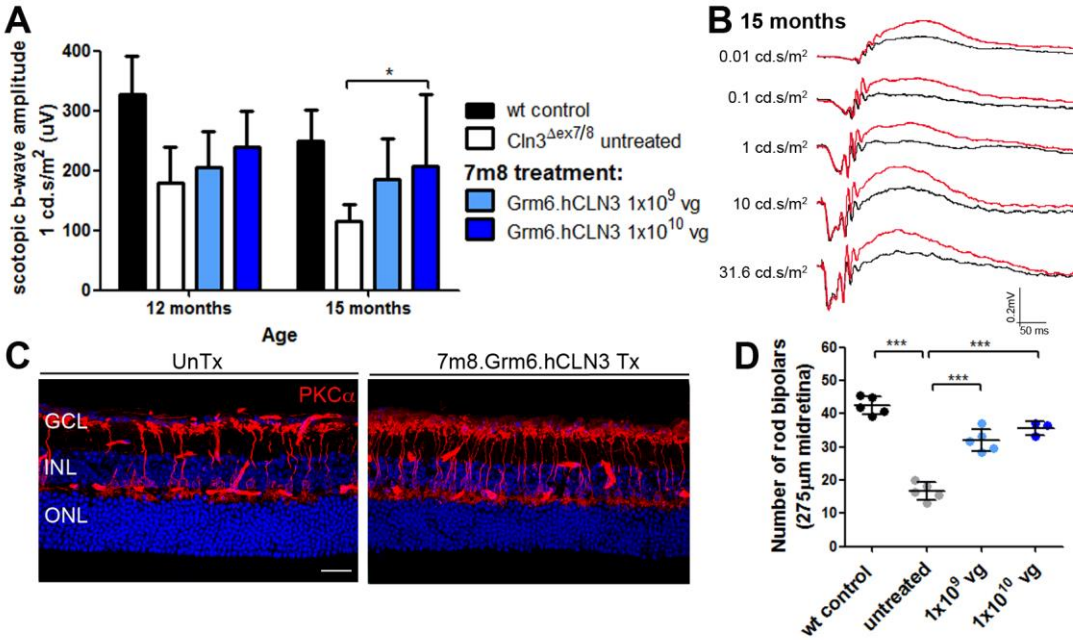

Figure 4: Bipolar cell-type specific expression of hCLN3 rescues the ocular phenotype of mutant mice (A) Scotopic ERG b-waves amplitudes of 7m8.Grm6.hCLN3-treated mutant mice. Wild type: n = 7-8 eyes, *Cln3*$^{\Delta ex7/8}$: n = 8-9 eyes, 7m8.CMV.hCLN3 1x10^{9} vg: n = 5-6 eyes, 7m8.CMV.hCLN3 1x10^{10} vg: 3-4 eyes. Wild type recordings from figure 1 were added as a reference. **(B)** Scotopic ERG traces of a mutant mouse that received treatment in one eye (red). The contralateral eye was left uninjected (black). **(C)** Representative confocal images of the mid-retina from untreated and a high titre 7m8.Grm6.hCLN3-treated eyes stained for PKCα at 15 months. **(D)** Counts of PKCα-positive cells in the mid-retina at 15 months. Data are presented as means ± SD and analysed by **(A)** two-way ANOVA with Bonferroni test and **(D)** one-way ANOVA with Kruskal Wallis test (*p < 0.05, ***p < 0.001). Scale bar: 25µm.

Supplementary information legends and tables:

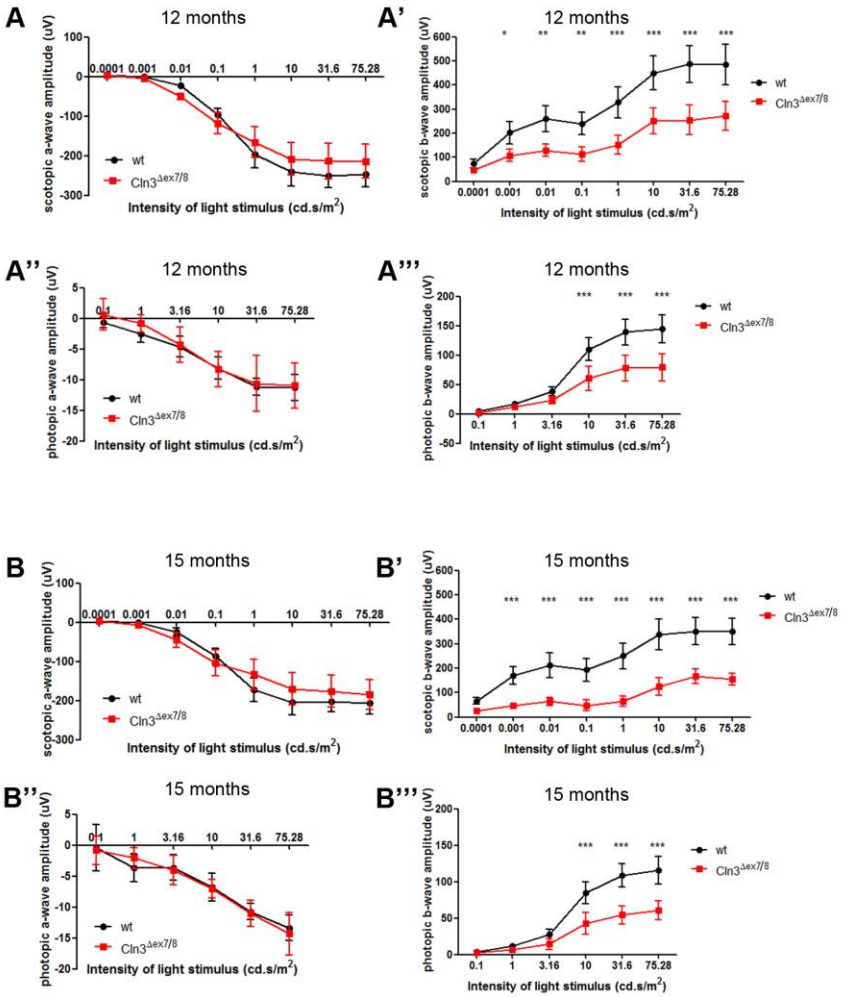

Figure S1: Full ERG analysis of *Cln3$^{\Delta ex7/8}$* and wild type mice over time

Scotopic and photopic ERG recordings at all light intensities at 12 months **(A-A'''')** and 15 months **(B-B''')** in *Cln3$^{\Delta ex7/8}$* and wild type mice. The scotopic and photopic b-wave amplitudes were significantly reduced in mutant mice compared with wild type controls at 12 and 15 months. No significant differences were detected in the scotopic and photopic a-wave amplitudes over time. Wild type: n = 7-8 eyes, *Cln3$^{\Delta ex7/8}$*: n = 6 eyes. Two-way ANOVA with Bonferroni test (*p < 0.05, **p < 0.01, ***p < 0.001).

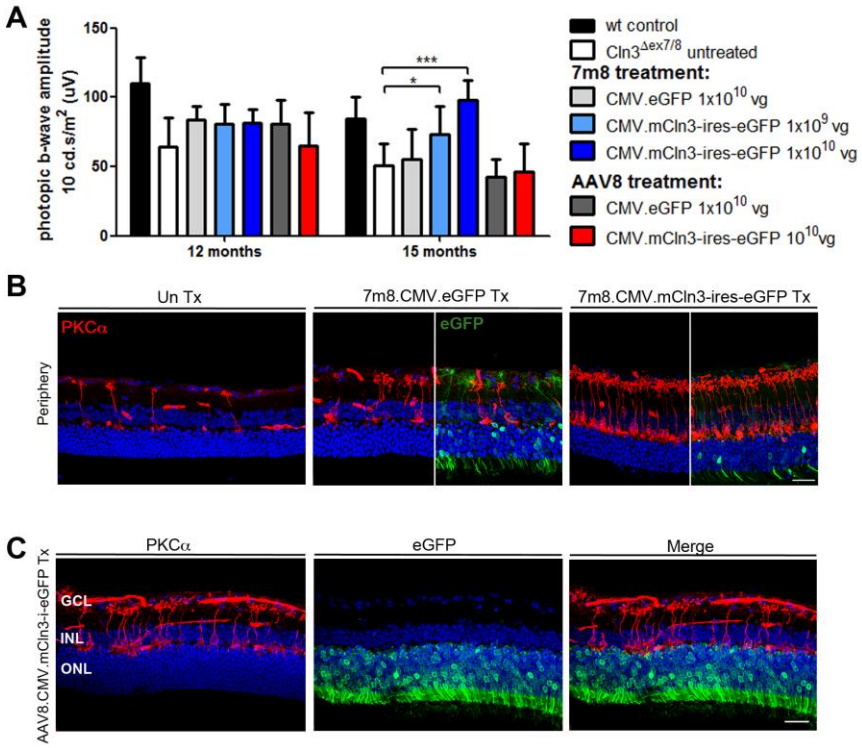

Figure S2: ERG recordings and retinal histology of treated mutant eyes

(A) Photopic b-wave amplitudes of *Cln3*$^{\Delta ex7/8}$ following intravitreal injections with 7m8.CMV.mCln3-ires-eGFP and subretinal injections with AAV8.CMV.mCln3-ires-eGFP. Wild type recordings from figure 1 were added as a reference. For n numbers see figure 2. Two-way ANOVA with Bonferroni test (*$p < 0.05$, ***$p < 0.001$). **(B)** Representative confocal images of the peripheral retina from untreated, 7m8.CMV.eGFP and 7m8.CMV.mCln3-ires-eGFP-treated retinas at 15 months. PKCα immunostaining demonstrates that the intravitreal delivery of mCln3 also had a therapeutic effect on the number of bipolar cells in the periphery compared with untreated or control-treated mutant retinas. **(C)** Representative confocal images of the mid-retina from AAV8.CMV.mCln3-ires-eGFP-treated retinas at 15 months. Immunostaining for eGFP reveals transduced photoreceptors. Staining for PKCα indicates that the treatment did not prevent the loss of rod bipolar cells, which is in line with the reduced ERG b-wave amplitudes in AAV8-treated retinas. Scale bar: 25µm.

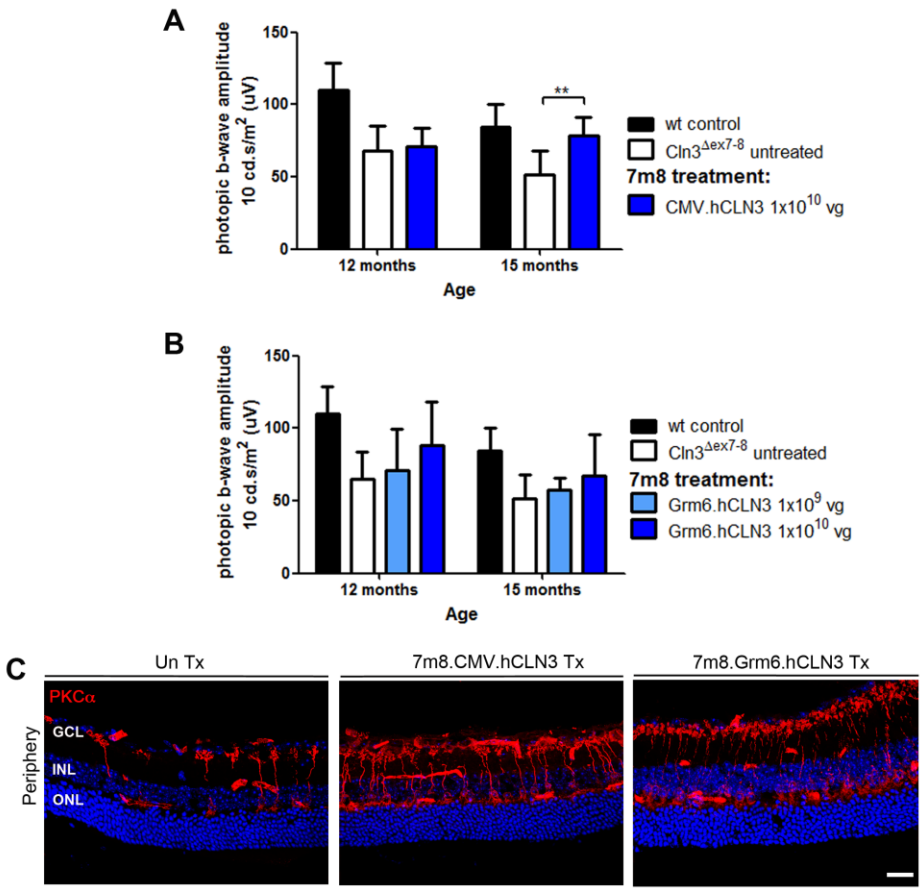

Figure S3: Photopic b-wave amplitudes of treated mutant mice and histological analysis of the periphery following 7m8.hCLN3 treatment

Photopic b-wave amplitudes of *Cln3*$^{\Delta ex7/8}$ mice that received intravitreal injections with 7m8.CMV.hCLN3 **(A)** and 7m8.Grm6.hCLN3 **(B)** at 12 and 15 months. 7m8.CMV.hCLN3 treatment resulted in significantly increased photopic b-wave amplitudes at 15 months, whilst 7m8.Grm6.hCLN3 treatment did not lead to higher b-wave amplitudes. Wild type recordings from figure 1were added as a reference . For n numbers see figure 3 and 4, respectively. Two-way ANOVA with Bonferroni test (**p < 0.01). **(C)** Representative images of the peripheral retina of untreated, 7m8.CMV.hCLN3 and 7m8.Grm6.hCLN3-treated mutant mice at 15 months. The number of PKCα-positive cells is increased in the treated compared with the untreated retinas. Scale bar: 25µm.

Table S1: Summary of scotopic b-wave amplitudes in *Cln3*$^{\Delta ex7/8}$ mice that received intravitreal and subretinal injection.

Overview of the means ±SD of the scotopic b-wave amplitudes (at 1 cd.s/m^2) in all AAV treated mutant mice over time. Untreated mutant and wild type controls were added as a reference from figure 2.

Mouse strain	AAV treatment	Titre (vg/eye)	Scotopic b-wave amplitudes (mean ± SD)	
			12M	15M
Cln3$^{\Delta ex7/8}$	7m8.CMV.Cln3-ires-eGFP	1x10^9	281.2 ± 48.4	192.3 ± 40.4
Cln3$^{\Delta ex7/8}$	7m8.CMV.Cln3-ires-eGFP	1x10^{10}	278 ± 65.1	283.9 ± 52.5
Cln3$^{\Delta ex7/8}$	7m8.CMV.hCLN3	1x10^{10}	253 ± 51.3	251.4 ± 73.1
Cln3$^{\Delta ex7/8}$	7m8.Grm6.hCLN3	1x10^9	204.5 ± 60	186.3 ± 67.4
Cln3$^{\Delta ex7/8}$	7m8.Grm6.hCLN3	1x10^{10}	239.2 ± 60	206.6 ± 121
Cln3$^{\Delta ex7/8}$	7m8.CMV.eGFP	1x10^{10}	174.2 ± 41.1	99.7 ± 27
Cln3$^{\Delta ex7/8}$	AAV8.CMV.mCln3-ires-eGFP	1x10^{10}	175.2 ± 54.5	109.3 ± 55.1
Cln3$^{\Delta ex7/8}$	AAV8.CMV.eGFP	1x10^{10}	172 ± 61.5	93 ± 40.6
Cln3$^{\Delta ex7/8}$	-	-	154.5 ± 37.4	79.9 ± 31.9
wild type	-	-	327.6 ± 64	249.5 ± 51.3

Table S2: Summary of photopic b-wave amplitudes in *Cln3*$^{\Delta ex7/8}$ mice that received intravitreal and subretinal injection.

Overview of the means ±SD of the photopic b-wave amplitudes (at 10 cd.s/m^2) in all AAV treated mutant mice over time. Untreated mutant and wild type controls were added as a reference from figure 2.

Mouse strain	AAV treatment	Titre (vg/eye)	Photopic b-wave amplitudes (mean ± SD)	
			12M	15M
Cln3$^{\Delta ex7/8}$	7m8.CMV.Cln3-ires-eGFP	1x10^9	80.8 ± 13.7	73.5 ± 20.2
Cln3$^{\Delta ex7/8}$	7m8.CMV.Cln3-ires-eGFP	1x10^{10}	81.1 ± 10.1	98.25 ± 14
Cln3$^{\Delta ex7/8}$	7m8.CMV.hCLN3	1x10^{10}	71 ± 12.8	78.5 ± 12.6
Cln3$^{\Delta ex7/8}$	7m8.Grm6.hCLN3	1x10^9	70.8 ± 28.8	57.5 ± 8.2
Cln3$^{\Delta ex7/8}$	7m8.Grm6.hCLN3	1x10^{10}	88 ± 30	67.5 ± 28
Cln3$^{\Delta ex7/8}$	7m8.CMV.eGFP	1x10^{10}	83.8 ± 9.4	55.6 ± 21.6
Cln3$^{\Delta ex7/8}$	AAV8.CMV.mCln3-ires-eGFP	1x10^{10}	65.2 ± 23.5	46.6 ± 19.9
Cln3$^{\Delta ex7/8}$	AAV8.CMV.eGFP	1x10^{10}	80.4 ± 17.8	42.3 ± 13.4
Cln3$^{\Delta ex7/8}$	-	-	64.2 ± 21	50.9 ± 15.2
wild type	-	-	110 ± 18.9	84.8 ± 15.2